

Testing general relativity with the multipole spectra of the SDSS luminous red galaxies

KAZUHIRO YAMAMOTO¹, TAKAHIRO SATO¹, GERT HÜTSI^{2,3}

¹*Department of Physical Sciences, Hiroshima University, Higashi-hiroshima, 739-8526, Japan*

²*Department of Physics and Astronomy, University College London, London, WC1E 6BT*

³*Tartu Observatory, EE-61602 Tõravere, Estonia*

As a test of general relativity on cosmological scales, we measure the γ parameter for the growth rate of density perturbations using the redshift-space distortion of the luminous red galaxies in the Sloan Digital Sky Survey (SDSS). Assuming the cosmological constant model, which matches the results of the WMAP experiment, we find $\gamma = 0.62 + 1.8(\sigma_8 - 0.8) \pm 0.11$ at 1-sigma confidence level, which is consistent with the prediction of general relativity, $\gamma \simeq 0.55 \sim 0.56$. Rather high value of $\sigma_8 (\geq 0.87)$ is required to be consistent with the prediction of the cosmological DGP model, $\gamma \simeq 0.68$.

Introduction – Modified gravity models, e.g., $f(R)$ gravity, TeVeS theory, DGP model, have been proposed as possible alternatives to the dark energy model. Although these models might not be complete, they pose ambitious challenges to the fundamental physics, suggesting one to go beyond the standard model. In fact, a lot of dark energy surveys are already under progress.^{1),2)} Testing the theory of gravity on cosmological scales will surely become one of the important objectives of these future large surveys.^{3),4),5),6)}

Measurement of the growth of density perturbations will be the key for testing the gravity theory.^{7),8),9),10),11),12),13),14),15)} Several authors have already investigated the growth of density perturbations as a way of constraining these theories.^{16),17),18)} In the future weak lensing statistics will be a promising probe of the density perturbations, while the redshift-space distortions may also be useful for constraining the growth rate of perturbations.^{19),20)} Recently, Guzzo, et al. have reported a constraint on the growth rate by evaluating the anisotropic correlation function of the galaxy sample from the VIMOS-VLT Deep Survey (VVDS).²¹⁾

The characteristic redshift of the VVDS galaxy sample is rather large. However, the survey area of the VVDS sample is small. This is a disadvantage in detecting the linear redshift-space distortions. In the present paper, we use the Sloan Digital Sky Survey (SDSS) luminous red galaxy (LRG) sample from the Data Release 5, whose survey area is around 5000 square degrees. In this letter, we present the results of the multipole power spectrum analysis for the SDSS LRG sample, and subsequently use it to measure the γ parameter for the growth rate of density perturbations. This gives a simple test of general relativity. Throughout this paper, we use the units where the light speed equals 1.

Measurement of the quadrupole spectrum – The (linear) growth rate is defined by

$f = d \ln D_1 / d \ln a$, where D_1 is the growth factor, and a is the scale factor. Due to the continuity equation of the matter density the linear velocity field is related to the time derivative of the matter density contrast, which itself is proportional to the growth factor D_1 . The peculiar velocity of galaxies contaminates the observed redshift, which leads to the difference in the radial position if the redshift is taken as the indicator of the distance. This causes the difference in the spatial clustering between redshift space and real space, which is called the redshift-space distortion. The power spectrum including the redshift-space distortion can be modeled as (e.g., 22)) $P(k, \mu) = (b(k) + f\mu^2)^2 P_{\text{mass}}(k) \mathcal{D}(k, \mu)$, where μ is the directional cosine between the line of sight direction and the wave number vector, $b(k)$ is the bias factor, $P_{\text{mass}}(k)$ is the mass power spectrum, $\mathcal{D}(k, \mu)$ describes the damping factor due to the finger of God effect.

Thus, the redshift-space distortion causes the anisotropy of the clustering amplitude depending on μ . The multipole power spectra are defined by the coefficients of the multipole expansion^{23),24)} $P(k, \mu) = \sum_{\ell=0,2,\dots} P_\ell(k) \mathcal{L}_\ell(\mu) (2\ell+1)$, where $\mathcal{L}_\ell(\mu)$ are the Legendre polynomials.*) The monopole $P_0(k)$ represents the angular averaged power spectrum and is usually what we mean by the power spectrum. $P_2(k)$ is the quadrupole spectrum, which gives the leading anisotropic contribution. The usefulness of the quadrupole spectrum for the dark energy is discussed in 25).

Within the linear theory of density perturbations, the ratio of the quadrupole to the monopole is given by $P_2(k)/P_0(k) = [4\beta/3 + 4\beta^2/7]/5[1 + 2\beta/3 + \beta^2/5]$, where $\beta = f/b(k)$. Thus, we can measure the growth rate from the quadrupole-monopole ratio. However, there are two difficulties to perform this method. The first is the clustering bias $b(k)$, for which we need other independent information. The second is the effect of nonlinear velocity, the finger of God effect, which significantly contaminates the quadrupole spectrum, as one can see in Figure 1-b.

In the present work we measured the monopole and quadrupole power spectra in the clustering of the SDSS DR5 luminous red galaxy sample. The galaxy sample used in our analysis consists of 64867 galaxies over the survey area of 4780 deg² and redshift range $0.16 \leq z \leq 0.47$.²⁶⁾ We have excluded the southern survey stripes since these just increase the sidelobes of the survey window without adding much of the extra volume. We have also removed some minor parts of the LRG sample to obtain more continuous and smooth chunk of volume.

The scheme to measure the monopole and the quadrupole spectrum is the same as the one described in reference 24). In this analysis we adopted the comoving distance of the fiducial model, which we assumed to be a flat universe with the cosmological constant and matter density parameter $\Omega_m = 0.3$. In our power spectrum analysis we fixed the weight function equal to 1.

Figure 1-a shows the monopole spectrum. The error bars correspond to the 1-sigma errors. The result is consistent with the previous measurement by Hütsi in reference 26), which is also plotted in this figure for comparison. As discussed in reference 26), the monopole spectrum reveals the baryon acoustic oscillation feature.

*) Note that our definition of the multipole spectrum $P_\ell(k)$ is different from the conventional definition by the factor $2\ell + 1$.

Figure 1-b plots the ratio of the quadrupole to the monopole. The quadrupole spectrum changes the signature at the wave number $k \sim 0.3 \text{ hMpc}^{-1}$. This is because the finger of God effect becomes significant on small scales. The solid curve is the theoretical curve for the Λ CDM model with $\Omega_m = 0.3$, $n_s = 0.96$ (initial spectral index), $\sigma_8 = 0.8$, $h = 0.7$, $\gamma = 0.56$ and $\sigma_v = 360 \text{ km/s}$ (see also below), and assumes a clustering bias $b(k) = 1.2[1 + 0.2(k/0.1 \text{ hMpc}^{-1})^{1/2}]$.

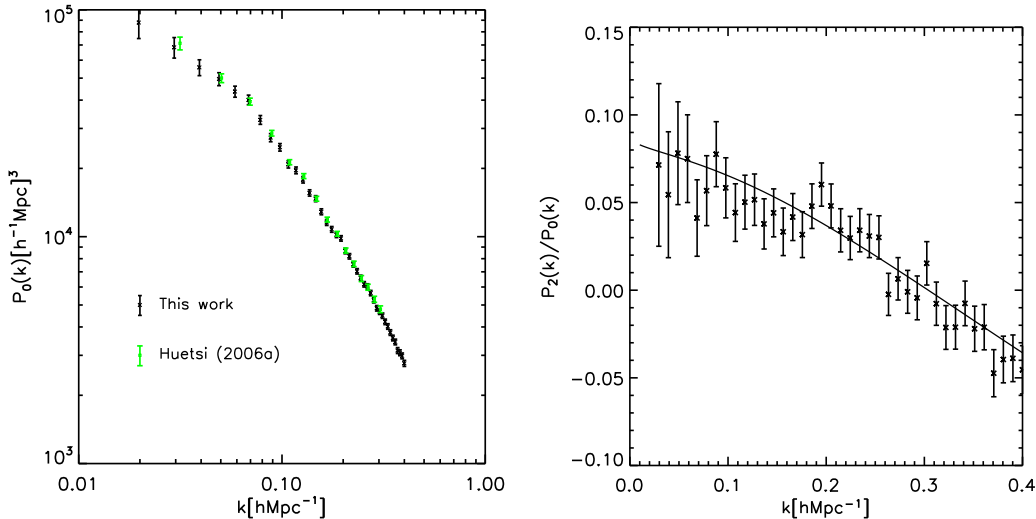


Fig. 1. (a, Left) Monopole power spectrum as a function of the wave number. The dark (black) points represent this work, the light (green) points the previous result.²⁶⁾ (b, Right) Quadrupole power spectrum divided by the monopole spectrum. The solid curve is the theoretical curve of the Λ CDM model.

Testing the growth rate – By using the quadrupole spectrum, we perform a simple test of the gravity theory. In particular, we focus on the γ parameter, which is introduced to parameterise the growth rate as, $f \equiv d \ln D_1(a)/d \ln a = \Omega_m(a)^\gamma$, where $\Omega_m(a) = H_0^2 \Omega_m a^{-3}/H(a)^2$, $H(a) = \dot{a}/a$ is the Hubble expansion rate, $H_0 (= 100 \text{ h km/s/Mpc})$ is the Hubble parameter.

Measurement of γ provides a simple test of the gravity theory. Within general relativity, even with the dark energy component, γ takes the value around $\gamma \simeq 0.55$.⁷⁾ However, γ may take different values in modified gravity models. For example, $\gamma \simeq 0.68$, in the cosmological DGP model including a self-acceleration mechanism. Thus, the measurement of γ is a simple test of general relativity.

As mentioned in the previous section, we need to take the clustering bias and the finger of God effect into account. For the finger of God effect we adopt the following form of $\mathcal{D}(k, \mu)$, the damping due to the nonlinear random velocity, $\mathcal{D}(k, \mu) = 1/[1 + (k\mu\sigma_v/H_0)^2/2]$, where σ_v is the one dimensional pairwise velocity dispersion (e.g., 29)). This form of the damping assumes an exponential distribution function for the pairwise peculiar velocity. In order to determine the clustering bias, we simply fix the value of σ_8 . If σ_8 is fixed, and the cosmological parameters and the clustering bias are given, we can compute the monopole spectrum $P_0^{\text{theor}}(k)$ with

$P_\ell(k) = \frac{1}{2} \int_{-1}^1 d\mu P(k, \mu) \mathcal{L}_\ell(\mu)$, where we use the Peacock and Dodds formula for the mass power spectrum $P_{\text{mass}}(k)$.²²⁾ We determine the clustering bias $b(k_i)$ through the condition $P_0^{\text{obs}}(k_i) = P_0^{\text{theor}}(k_i)$ using a numerical method. Here $P_0^{\text{obs}}(k_i)$ is the measured value of the monopole at wave number k_i , and $P_0^{\text{theor}}(k_i)$ is the corresponding theoretical value. Figure 2 exemplifies the bias obtained by the above method for the cases of σ_8 fixed as $\sigma_8 = 0.9, 0.8, 0.7$.

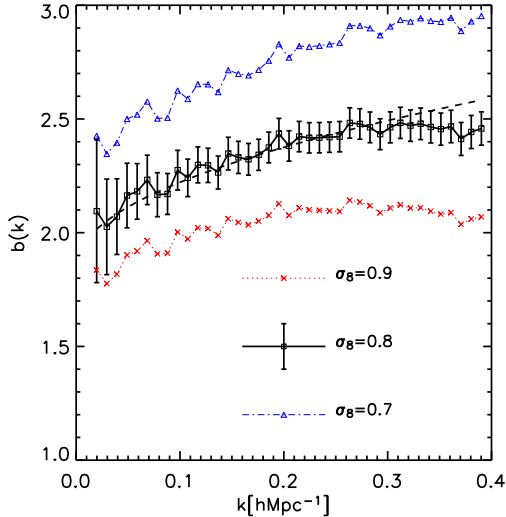


Fig. 2. The bias $b(k_i)$ obtained from our numerical method. The three curves correspond to $\sigma_8 = 0.9, 0.8, 0.7$ and the other parameters are the same as those of Figure 1-b. For the case $\sigma_8 = 0.8$ the errors are estimated from those of $P(k_i)$. The dashed curve is $b(k) = 1.2[1 + 0.2(k/0.1h\text{Mpc}^{-1})^{1/2}]$.

curves assume $\sigma_8 = 0.8$, while the dotted (dashed) ones $\sigma_8 = 0.7$ ($\sigma_8 = 0.9$). The other parameters are fixed as $\Omega_m = 0.28$,^{*)} $n_s = 0.96$, $h = 0.7$.³¹⁾ In Figure 3-a we plot the contour levels of $\Delta\chi^2 = 2.3$ (inner curves) and 6.2 (outer curves), which correspond to the 1-sigma and 2-sigma confidence levels of the χ^2 distribution. Clearly, the higher value of σ_8 favours higher value for γ . We find $\gamma = 0.62 + 1.8(\sigma_8 - 0.8) \pm 0.11$ (± 0.19) and $\sigma_v = 367 + 80(\sigma_8 - 0.8) \pm 16$ (± 27) km/s at 68 (90) percent confidence level, respectively. The value of γ is consistent with general relativity. The result is not sensitive to the inclusion of the baryon oscillation in the theoretical power spectrum.

The relation of γ and σ_8 can be understood as the degeneracy between σ_8 and the growth rate f in the following way. As the observed power spectra can be roughly written as $P_0^{\text{obs}} \propto b^2(k)\sigma_8^2 D_1^2(z)/D_1^2(z=0)$ and $P_2^{\text{obs}} \propto b(k)f\sigma_8^2 D_1^2(z)/D_1^2(z=0)$,

We used the monopole spectrum to determine the bias, and the quadrupole spectrum to obtain constraints on γ and σ_v . Since the galaxy sample covers rather broad redshift range, $0.16 \leq z \leq 0.47$, the effect of the time-evolution (light-cone effect) should be considered properly.³⁰⁾ However, for simplicity, we here evaluated the theoretical spectra at the mean redshift of $z = 0.31$.

Figure 3-a demonstrates the contours of $\Delta\chi^2$ in the γ versus σ_v parameter plane. We compute χ^2 as $\chi^2 = \sum_i [P_2^{\text{obs}}(k_i) - P_2^{\text{theor}}(k_i)]^2 / [\Delta P_2^{\text{obs}}(k_i)]^2$, where $P_2^{\text{obs}}(k_i)$ and $\Delta P_2^{\text{obs}}(k_i)$ are the measured values and errors as plotted in Figure 1-b. $P_2^{\text{theor}}(k_i)$ are the corresponding theoretical values. The solid

*) As the observed power spectra are obtained by adopting the distance-redshift relation of the fiducial model, the flat Λ CDM model with $\Omega_m = 0.3$, the cosmological distortion effect is taken into account properly in our theoretical computation.^{27), 28)}

the degeneracy between σ_8 and the growth rate f (or γ) in our method is given by $f\sigma_8 D_1(z)/D_1(z=0) = \text{constant}$.

Figure 3-b is the analogue of Figure 3-a, with the expansion history now taken to be that of the spatially flat DGP model, which follows $H^2(a) - H(a)/r_c = 8\pi G\rho/3$, where ρ is the matter density and $r_c = H_0/(1 - \Omega_m)$ is the crossover scale related to the 5-dimensional Planck mass. The expansion history in this model can be well approximated by the dark energy model with the equation of state parameter $w(a) = w_0 + w_a(1-a)$, where $w_0 = -0.78$ and $w_a = 0.32$, as long as $\Omega_m \sim 0.3$.⁷⁾ However, the Poisson equation is modified, and the growth history is approximated by the formula with $\gamma \simeq 0.68$. In order to be consistent with $\gamma = 0.68$, Figure 3-b requires higher value of σ_8 as compared to the Λ CDM case. We find $\gamma = 0.47 + 1.7(\sigma_8 - 0.8) \pm 0.09$ at 68 percent confidence level, which requires $\sigma_8 \geq 0.87$.

The pair-wise velocity dispersion measured in this work is somewhat smaller than the theoretical model in the reference.²⁹⁾ Li, et al. investigated the pair-wise velocity of the SDSS galaxies.³²⁾ Their analysis is limited since it is based on galaxies with redshifts less than 0.3, however, they report the dependence of the pairwise velocity dispersion on galaxy properties and also on scales.

Conclusion – In summary, we measured the monopole and quadrupole spectra in the spatial clustering of the SDSS LRG galaxy sample from DR5. The monopole spectrum is consistent with the previous result by Hütsi. Using the quadrupole spectrum, we measured the γ parameter for the linear growth rate and the pair-wise peculiar velocity dispersion. The measurement of γ provides a simple test of general relativity. The measured value of γ is consistent with general relativity, however, it is inconsistent with the cosmological DGP model, $\gamma \simeq 0.68$, as long as $\sigma_8 < 0.87$. If a constraint on σ_8 from other independent sources, e.g., the cosmic microwave background anisotropies, is included, we would be able to obtain tighter constraint on the DGP model.³³⁾ The constraint on γ can be applied to other modified gravity models, given that the value of γ which characterizes a particular model is found, as discussed by Linder and Cahn³⁴⁾ (cf.³⁵⁾). In this work we only considered a spatially flat model and fixed the cosmological parameters so as to match with the results of the WMAP experiment. The constraint on γ will be weakened by including the uncertainties of the cosmological model, e.g., the dark energy properties.

Acknowledgements We would like to thank H. Nishioka, Y. Kojima and Y. Suto for useful discussions and comments. We thank G. Nakamura, K. Koyama and R. C. Nichol for useful comments and discussions on the earlier version of the manuscript. This work was supported by a Grant-in-Aid for Scientific research of Japanese Ministry of Education, Culture, Sports, Science and Technology (No. 18540277).

References

- 1) A. Albrecht, et al., arXiv:astro-ph/0609591
- 2) J. A. Peacock, et al., arXiv:astro-ph/0610906
- 3) D. Huterer, E. V. Linder, Phys. Rev. D **75** (2007), 023519
- 4) M. Ishak, A. Upadhye, D. N. Spergel, Phys. Rev. D **74** (2006), 043513
- 5) K. Yamamoto, B.A.Bassett, R.C.Nichol, Y.Suto, K.Yahata Phys. Rev. D **74** (2006), 063525

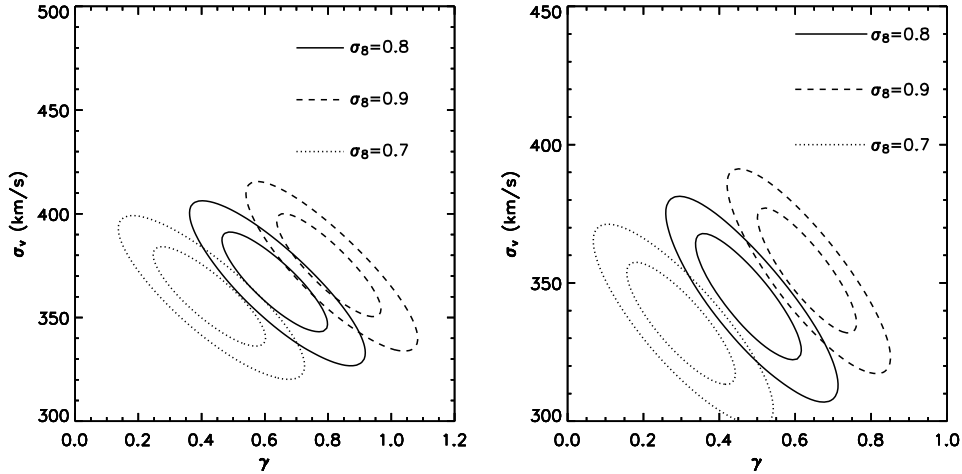


Fig. 3. (a, Left) $\Delta\chi^2$ in the γ - σ_v plane. We fixed the normalization of the mass power spectrum as $\sigma_8 = 0.7$ (dotted curves), $\sigma_8 = 0.8$ (solid curves), and $\sigma_8 = 0.9$ (dashed curves), respectively. The contour levels are $\Delta\chi^2 = 2.3$ (inner curves) and 6.2 (outer curves), which correspond to the 1-sigma and 2-sigma confidence levels of the χ^2 distribution. The other parameters are fixed as $\Omega_m = 0.28$, $n_s = 0.96$, and $h = 0.7$.³¹⁾ (b, Right) Same as the left (a), except here we used the expansion history of the DGP model.

- 6) K.Yamamoto, D.Parkinson, T.Hamana, R.C.Nichol, Y.Suto Phys. Rev. D **76** (2007), 023504
- 7) E. V. Linder, Phys. Rev. D **72** (2005), 043529
- 8) L. Amendola, et al., Journal of Cosmology and Astroparticle Physics 04 (2008), 013
- 9) A. F. Heavens, T. D. Kitching, L. Verde, MNRAS 380 (2007), 1029.
- 10) K. Koyama, R. Maartens, Journal of Cosmology and Astroparticle Physics 01 (2006), 016
- 11) M. Kunz, D. Sapone, Phys. Rev. Lett. **98** (2007), 121301
- 12) B. Jain, P. Zhang, arXiv:0709.2375
- 13) T. Chiba, T. Nakamura, Prog. Theor. Phys. **118** (2007), 815
- 14) Y.-S. Song, K. Koyama, arXiv:0802.3897
- 15) J-P. Uzan, arXiv:astro-ph/0605313
- 16) S. Nesseris, L. Perivolaropoulos, Phys. Rev. D **77** (2008), 023504
- 17) C. di Porto, L. Amendola, Phys. Rev. D **77** (2008), 083508
- 18) Y. Wang Journal of Cosmology and Astroparticle Physics, in press, 2007arXiv:0710.3885
- 19) E. V. Linder, arXiv:0709.1113
- 20) D. Sapone, L. Amendola, arXiv:0709.2792
- 21) L. Guzzo, et al., Nature **451** (2008), 541
- 22) J. A. Peacock, S. J. Dodds, MNRAS 280 (1996), L19; MNRAS 267 (1994), 1020
- 23) A. N. Taylor, A. J. S. Hamilton, MNRAS 282 (1996), 767
- 24) K. Yamamoto, et al., Publications of the Astronomical Society of Japan 58 (2006), 93
- 25) K. Yamamoto, B. A. Bassett, and H. Nishioka Phys. Rev. Lett. **94** (2005), 051301
- 26) G. Hütsi, A&A 449 (2006), 891; A&A 459 (2006), 375
- 27) W. E. Ballinger, J. A. Peacock, A. F. Heavens, MNRAS 282 (1996), 877
- 28) T. Matsubara, Y. Suto, Astrophysical Journal 470 (1996), L1
- 29) H. J. Mo, Y. P. Jing, G. Boerner, MNRAS 286 (1997), 979
- 30) K. Yamamoto, Y. Suto, Astrophysical Journal 517 (1999), 1
- 31) E. Komatsu, et al., arXiv:0803.0547
- 32) C. Li, et al., MNRAS 368 (2006), 37
- 33) A. Lue, R. Scoccimarro, G. D. Starkman, Phys.Rev. D69 (2004), 124015
- 34) E. V. Linder, R. N. Cahn, Astroparticle Physics 28 (2007), 481
- 35) D. Polarski, R. Gannouji, arXiv:0710.1510; R. Gannouji, D. Polarski, arXiv:0802.4196